ITEP-23-94

Fermilab Library
0 1160 0037133 0

INSTITUTE OF THEORETICAL
AND EXPERIMENTAL PHYSICS

ITEP-23-94

A.E.Kudryavtsev , B.L.Druzjinin

The determination of the strong $\bar{N}N$-scattering lengths and the solution for the problem of the real-to-imaginary ratio of the forward elastic $\bar{p}p$- scattering amplitude

FERMILAB
JUN 28 1994
LIBRARY

MOSCOW 1994

UDK 539.17 M-16

THE DETERMINATION OF THE STRONG $\bar{N}N$-SCATTERING LENGTHS AND THE SOLUTION FOR THE PROBLEM OF THE REAL-TO-IMAGINARY RATIO OF THE FORWARD ELASTIC $\bar{p}p$-SCATTERING AMPLITUDE: Preprint ITEP 23-94/

A.E.Kudryavtsev*, B.L.Druzjinin - M., 1994 - 16p.

An analysis of the recent OBELIX $\bar{n}p$-total and annihilation cross-sections is performed in terms of scattering length approximation. The extracted isospin $I = 1$ $\bar{N}N$-scattering length considered together with the $\bar{p}p$- scattering length provides possibility to get the $I = 0$ $\bar{N}N$-scattering length. The isospin violation seemed to be essential and is introduced kinematically. The solution reproduces the known low-energy $\bar{p}p$-annihilaton cross-section at 70 MeV/c. The real-to-imaginary ratio of the forward $\bar{p}p$-elastic amplitude changes its sign near the $\bar{n}n$-threshold. Some predictions for total, annihilation, elastic and charge-exchange cross-sections are also given.

Fig. - 4, ref. - 15

© Институт теоретической и экспериментальной физики, 1994

*e-mail:KUDRYAVTSEV@VXITEP.ITEP.MSK.SU

1.Analysis of the $\bar{n}p$-data at very low energy

Recently the measurement of the $\bar{n}p$-total and annihilation cross-sections was performed in a relatively wide momentum range $(70 \div 240)$ MeV/c [1]. The data at 70 and 100 MeV/c are of great interest for the present analysis because they contain information on the isospin $I = 1$ $\bar{N}N$-scattering amplitude. One may think that at very low energy S-wave scattering dominates. Considering the experimental results from the ref. [1], we conclude that the data at $p_{lab} = 70$, 100 and 120 MeV/c are not in contradiction with the S-wave scattering mechanism. But to describe the points above 120 MeV/c one definitely needs some admixture of the P-wave. So later on we shall restrict our attention by the points below 140 MeV/c and shall use the S-wave approach. Notice that at very low energies the zero effective range approximation may be used,

$$f_1 = \frac{1}{a_1 - ib_1 - ik}, \tag{1}$$

where the index 1 denotes isospin, a_1 and b_1 are constants, $b_1 > 0$ and k is the c.-m. momentum, $k = p_{lab}/2$. Taking as input the values of σ^{tot} and σ^{ann} at $p_{lab} = 70$ and 100 MeV/c from the ref. [1], we get the best fit for these observables if the parameters a_1 and b_1 are:

$$a_1 = \pm 0.2884, b_1 = 0.1084 \tag{2}$$

Notice that the sign of a_1 can not be determined from the data on the $\bar{n}p$ scattering. Using the numbers from the eq.(2), we get the $\bar{n}p$ cross-sections,which are tabulated in the Table 1 and are shown in the Figure 1.Using the numbers from the eq.(2) we get the following $\bar{n}p$-scattering length:

$$A_1 = (\pm 3.04 + i1.14) fm \tag{3}$$

Sign(+) in eq.(3) corresponds to effective attraction in $\bar{n}p$-system and vice versa.From the eq. (3) we get,that

$$\lim_{k\to 0} \beta\sigma^{tot}_{\bar{n}p} = \lim_{k\to 0} \beta\sigma^{ann}_{\bar{n}p} = 60.2mb. \tag{4}$$

2.The $\bar{p}p$-scattering case

The $\bar{p}p$-Coulomb-modified scattering length A_c, is determined from the shift and the width of the $1s$-level of the $\bar{p}p$-atom. The purely hadronic

scattering length A_s is connected with A_{cs} by the well-known Schwinger formula [2]. In connection with the $\bar{p}p$-case the relation between A_s and A_{cs} was reconsidered carefully in the paper [3]. In what follows we shall use the results for A_s from the recent papers [4] and [5].

One may get the expression for the purely hadronic $\bar{p}p$-scattering amplitude $f^s_{\bar{p}p}$ using the two-channel formalism, developed long ago in the paper [6], see also more recent paper [7]. In the notations of the ref. [7] the elastic $\bar{p}p$-amplitude has the form:

$$f^s_{\bar{p}p}(k) = (\alpha_{22} - ip)/((\alpha_{11} - ik)(\alpha_{22} - ip) - \alpha_{12}\alpha_{21}) \tag{5}$$

If isospin is not violated dynamically, the matrix elements α_{ij} of the $\hat{M}$-matrix ,$\hat{T} = (\hat{M} - i\hat{p})^{-1}$,are related to scattering lengths $A_{0,1}$ of definite isospin,see,e.g.,refs. [8]:

$$\alpha_{11} = \alpha_{22} = \frac{1}{2}(\frac{1}{A_0} + \frac{1}{A_1}) \tag{6a}$$

$$\alpha_{12} = \alpha_{21} = \frac{1}{2}(\frac{1}{A_0} - \frac{1}{A_1}) \tag{6b}$$

In the eqs. (6a) and (6b) k and p are centre of mass momenta for the $\bar{p}p$- and the $\bar{n}n$-systems correspondingly. Notice, that below the $\bar{n}n$ -threshold the momentum p becomes purely imaginary. Considering the equation (5) at $k = 0$,one may get the relation between the purely hadronic $\bar{p}p$-scattering length A_s and the scattering lengths A_1 and A_0. So we may find the value A_0 from this relation. It is presented in the Table 2. The tree different variants of A_s, entering the Table 2, are taken from the reference [4]. The first row in that Table corresponds to the shift and width of the $^1S_0$-atomic state.The second row is the mean value among the four spin averaged quantities for A_s,mentioned in the ref. [4].The last row refers to the PS175 experiment, which determined mostly the triplet $^3S_1$ width and shift.In the Table 3 we also give results for $\beta\sigma^{ann}_{\bar{p}p}$ at 70 MeV/c,which follow from our consideration. The experimental result for this quantity is [9]:

$$\beta\sigma^{ann}_{\bar{p}p}(p_{lab} = 70MeV/c) \approx (33.2 \pm 1.7 \pm 1.8)mb \tag{7}$$

Looking at the Table 2, we conclude, that the result of the calculation for $\beta\sigma^{ann}_{\bar{p}p}$ at 70 MeV/c depends crucial on the choice of A_s.The today's experimental situation is in agreement with the choice of A_s as being taken from the experiment with protonium in the $^3S_1$-state. So one may

think that the main contributions to both $\bar{n}p$- and $\bar{p}p$ -cross-sections at very low energies come from the triplet scattering.

Here we have to mention that solutions, presented in the Table 2, have positive sign of real part of A_1.We were not able to find the solutions for A_0 consistent with the unitarity condition,if $ReA_1 < 0$.The results of calculations for the $\bar{p}p$-cross-sections[1] with A_s from the third row of the Table 2, are presented in the Table 3 and are shown in the Figure 2. We see from this Figure, that cross-sections have some irregularities, evidently connected with the $\bar{n}n$-threshold.

3.The behaviour of the real-to-imaginary ratio of the $\bar{p}p$-elastic forward scattering amplitude

Results of the paper [10] for the function $\rho(E) = Ref_{\bar{p}p}(0°)/Imf_{\bar{p}p}(0°)$ still remain a puzzle. The attempts to describe the behaviour of $\rho(E)$ with usual optical potential models were unsuccessful, see, e.g. the paper [11]. Notice, that the routine fit in the effective range approximation based on data above the momentum 180 MeV/c also reproduces the behaviour of $\rho(E)$ unsatisfactory [12].

Looking at the Table 3,we realize,that in our approach the function $\rho(E)$ changes its sign just near the $\bar{n}n$- threshold. So the unexpected sharp behaviour of $\rho(E)$ is linked with the presence of the second $\bar{n}n$-channel in the $\bar{p}p$-problem.This was the main point of the explanation for the $\rho(E)$ behaviour, given in the paper [13].But as follows from our consideration,the sharp dependence of $\rho(E)$ is connected not only with the $\bar{n}n$-threshold by itself, but also with some special relation between the two scattering lengths,A_0 and A_1,which follows from the condition:

$$| Re\alpha_{11} | \ll | Re\alpha_{12} | \qquad (8)$$

The inequality (9) takes place in our case as both A_0 and A_1 have relatively large values of real parts but of opposite signs.Under this condition the isospin breaking is enhanced and provides the changing of the sign of the real part of the $\bar{p}p$-scattering amplitude.In the Figure 3 we give as an illustration the Argand plot for the purely hadronic $\bar{p}p$- scattering amplitude in the momentum range $0 \leq p_{lab} \leq 140$ MeV/c.

[1]In the Tables 3 and 4 we give the Coulomb corrected cross-sections

4.The charge-exchange $\bar{p}p \to \bar{n}n$ reaction

Knowing A_0 and A_1, we may calculate cross-sections for any $\bar{N}N$ system. It is useful to clarify the situation with the charge exchange $\bar{p}p \to \bar{n}n$ reaction. The cross-section for this reaction is a crucial point of the proposed theoretical scenario as for $p_{lab} \geq 180$ MeV/c it is known to be small,much smaller than the elastic cross section at the same energy. The results of the calculation for the S-wave part of the total charge-exchange cross-section are given in the Table 4, see also Figure 4. From this Table we see that the S-wave part of the charge-exchange cross-section is smaller than the experimental value [14]:

$$\sigma_{CE} = (12.5 \pm 1.5)mb \tag{9}$$

So our solution is not in contradiction with the today's experimental situation for charge-exchange cross-section as well. Notice, that we predict the existence of maximum for this cross section near the momentum 120 MeV/c. So it would be desirable to check experimentally our predictions for σ_{CE}.

5.Concluding remarks

i) The presented phenomenological analysis of the low-energy $\bar{N}N$-problem is based on the current experimental situation for the $\bar{n}p$-cross-sections [1]. So the parameters, extracted from our analysis, may be changed if the $\bar{n}p$ data will be changed. But the whole picture for $\bar{n}p$,$\bar{p}p$, $\bar{p}p$-atom and the $\rho(E)$ behaviour seems to be selfconsistent. So one may hope,that in the future experiments we shall not get drastical changes for all the $\bar{n}p$- and $\bar{p}p$-cross sections in this low-energy region.

ii)Our analysis is based on formulae for spinless particles. The main reason for this approach is a real absence of any polarization experiment in this region excluding some atomic data. Nevertheless we managed to get some indirect information that the observed structure comes mainly from the triplet $\bar{p}p$-states of both isospin.

iii)The observed sharp beak-like behaviour of the proton formfactor near the threshold in the time-like region [15] is probably connected with the energy behaviour of the $\bar{p}p$-scattering amplitude. This is in agreement with the statement, that the puzzle takes place in the case of triplet $^3S_1$ state.

iv)We are not going to discuss here in details the singularities of the

$\bar{N}N$-amplitudes as some numericals,taken as input in our consideration, may be changed. Nevertheless using the today's experimental data on the $\bar{n}p$-cross-sections, we get a pole for the $\bar{n}p$-scattering amplitude. It corresponds to virtual (antibound) state, shifted into the complex plane via the presence of absorption. So we get an effective attraction in the isospin $I = 1$ triplet state. On contrary as it follows from the Table 2, for isospin $I = 0$ we definitely get repulsion.

We are grateful to K.G.Boreskov, C.Guaraldo, B.O.Kerbikov, V.G.Ksenzov and P.E.Volkovitsky for useful discussions.

Table 1

$p_{lab}(MeV/c)$	σ^{el}	σ^{tot}	σ^{ann}	$\beta\sigma^{tot}$	$\beta\sigma^{ann}$
20	1158	3636	2477	77.4	52.7
40	988	2045	1057	87.1	45.0
60	832	1425	593	91.1	37.9
70	762	1228	466	91.6	34.7
80	698	1071	373	91.3	31.8
90	639	944	304	90.5	29.1
100	587	838	251	89.2	26.7
110	539	748	210	87.7	24.5
120	496	673	177	86.0	22.6

The $\bar{n}p$-cross-sections (mb).

Table 2

A_s,fm	A_0,fm	$\beta\sigma^{ann}_{\bar{p}p}$ at 70 MeV/c
$-0.82+i1.27(^1S_0)$	$-1.99+i0.97$	51.4 mb
$-0.88+i0.84$ spin averaged	$-2.00+i0.60$	40.0 mb
$-1.17+i0.63(^3S_1)$	$-2.23+i0.42$	31.8 mb

Table 3

p_{lab}	$E_{c.m.}$	σ^{el}	$\beta\sigma^{tot}$	$\beta\sigma^{ann}$	ρ
20	0.107	1183	86.0	60.8	−1.60
40	0.426	436	58.4	39.8	−1.36
60	0.959	232	48.2	33.3	−1.11
70	1.306	167.1	44.3	31.8	−0.95
80	1.705	114.4	40.8	31.0	−0.73
90	2.158	74.8	38.3	31.1	−0.37
100	2.664	141.3	54.4	39.4	0.24
110	3.224	213.6	68.7	43.7	0.07
120	3.837	240.3	73.1	42.3	0.02

The $\bar{p}p$-cross-sections (in mb) and the ratio $\rho = Ref_{\bar{p}p}(0°)/Imf_{\bar{p}p}(0°)$. The energy $E_{c.m.}$ is given in MeV, the threshold energy $E_{th} = 2.6$MeV.

Table 4

p_{lab}(MeV/c)	$\sigma_{CE}(mb)$
100	9.9
110	19.2
120	19.4
130	18.0
140	16.2
150	14.4
160	12.7
170	11.1
180	9.8

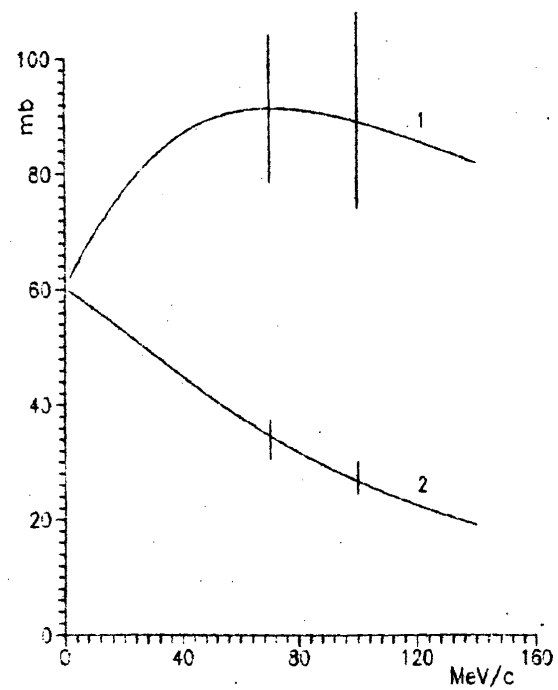

Fig.1. The $\bar{n}p$-total and annihilation cross-sections (in mb). Curve 1 corresponds to $\beta\sigma^{tot}$, curve 2 to $\beta\sigma^{ann}$. Experimental data are taken from ref. [1]

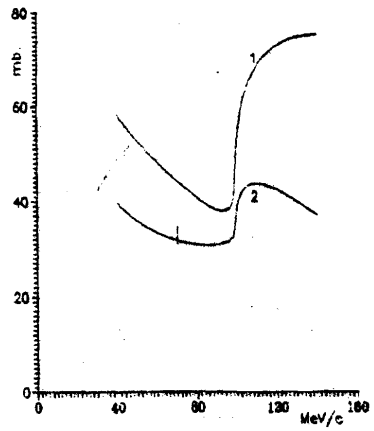

Fig.2a.The $\bar{p}p$-total and annihilation cross-sections (mb).Curve 1 corresponds to $\beta\sigma^{tot}$,curve 2 to $\beta\sigma^{ann}$.Experimental cross-section at p_{lab} = 70MeV/c is from ref.[9].

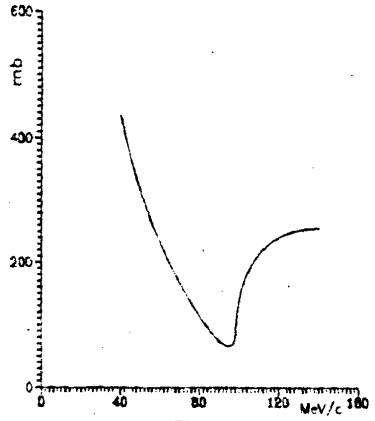

Fig.2b.The $\bar{p}p$-elastic cross-section.

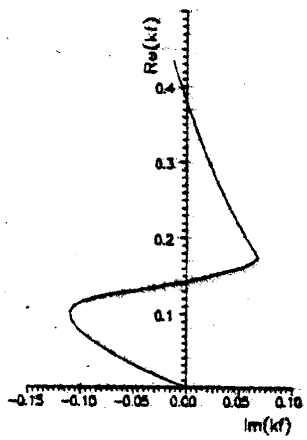

Fig.3a.The Argand diagram for the $\bar{p}p$ strong elastic scattering amplitude.

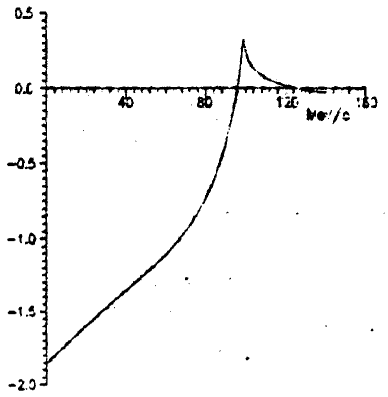

Fig.3b.The function $\rho(E) = Re f_{pp}/Im f_{pp}$.

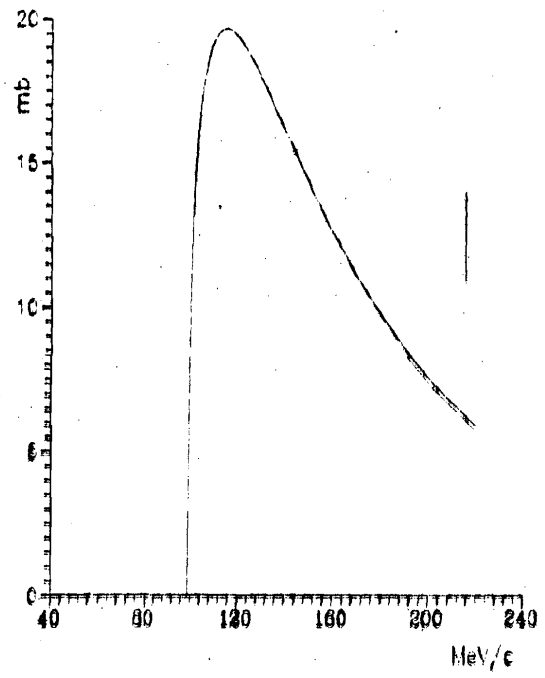

Fig.4.The *S*-wave contribution to the charge-exchange cross-section,in mb.Experimental cross-section at $p = 183$ MeV/c is from *ref.*[14]

References

[1] A.Adamo et al.,Nucl.Phys.,A558(1993)137c.

[2] J.Schwinger,Phys.Rev.,72(1947)724.

[3] V.S.Popov et al.,ZhETP,80(1981)1271;88(1985)715.

[4] J.Carbonell and K.V.Protasov. J.Phys.G:Nucl.Part.Phys.,18(1992)1863.

[5] C.J.Batty "Antiproton-Nucleon and Antiproton-Nucleus Interactions" Edited by F. Bradamante et al. Plenum Press, New York, 1990. p.251.

[6] R.Dalitz and S.F.Tuan, Ann. Phys.,10(1960)307.

[7] V.D.Mur, A.E.Kudryavtsev, V.S.Popov. Pis'ma v JETP, 31 (1980)429.

[8] I.L.Grach, B.O.Kerbikov, Yu.A.Simonov. Sov. J. Nucl. Phys.,48 (1988)609.

[9] M.Angello et al., Phys.Lett.,B256(1991) 349.

[10] W.Bruckner et al.,Phys.Lett.,158B (1985) 180.

[11] M.Lacombe, B.Loiseau et al.,Phys.Rev.Lett.,48(1982)1319.

[12] H.-J.Pirner, B.Kerbikov, J.Mahalanabis, Z. Phys.,A338(1991)111.

[13] O.D.Dalkarov and K.V.Protasov, Pis'ma v JETP ,44(1986)496.

[14] W.Bruckner et al., Phys.Lett.,189B (1987)223.

[15] G.Bardin et al.,Phys.Lett.,B255 (1991)1411.